Photochemical & Photobiological Sciences

ROYAL SOCIETY OF CHEMISTRY

PAPER

View Article Online
View Journal | View Issue

Cite this: *Photochem. Photobiol. Sci.*, 2020, **19**, 193

Curcumin derivatives as photosensitizers in photodynamic therapy: photophysical properties and *in vitro* studies with prostate cancer cells

K. T. Kazantzis,[a] K. Koutsonikoli,[a] B. Mavroidi,[b] M. Zachariadis,[c] P. Alexiou,[b] M. Pelecanou,[b] K. Politopoulos,[a] E. Alexandratou *[a] and M. Sagnou*[b]

Photodynamic therapy (PDT) is a minimally invasive approach to treat various forms of cancer, based on the ability of certain non-toxic molecules (photosensitizers) to generate reactive oxygen species (ROS) after excitation by light of a certain wavelength and eventually induce strong phototoxic reactions against malignant cells and other pathogens. Curcumin is one of the most extensively investigated phytochemicals with a wide range of therapeutic properties and has been shown to induce strong photocytotoxic effects in micromolar concentrations against a variety of cancer cell lines. Curcumin (**1**) is comparatively evaluated with the naturally occurring bisdemethoxy Curcumin (**2**), which lacks the two methoxy groups, as well as two newly synthesized curcuminoids, the cinnamaldehyde derivative (**3**) and the dimethylamino one (**4**), designed to increase the absorption maximum and hence the tissue penetration. The synthetic curcuminoids were successfully synthesized in sufficient amounts and their photophysical properties such as absorption, fluorescence, photobleaching and free radical generation were investigated. Compound **4** exhibited a significant increase in peak absorption (497 nm) and strong fluorescent emission signals were recorded for all curcuminoids. Photobleaching of **4** was comparable to **1** whereas **2** and **3** showed more extended photobleaching but much higher ROS production in very short irradiation times. Compounds **2** and **4** exhibited specific intracellular localization. After dark and light cytotoxicity experiments against LNCaP prostate cancer cell line for all curcuminoids, concentration of 3 μM and irradiance of 6 mW cm^{-2} were selected for the PDT application which resulted in remarkable results with very short LD_{50}. Curcuminoids **2** and **4** exhibited a significant dose-dependent PDT effect. The biphasic dose–response photodynamic effect observed for **1** and **3** may provide a strategy against prolonged and sustained photosensitivity.

Received 9th September 2019,
Accepted 8th January 2020

DOI: 10.1039/c9pp00375d

rsc.li/pps

Introduction

Photodynamic therapy (PDT), although is one of the most recently introduced therapeutic modalities, has already been successful in presenting a considerable number of approved therapeutic protocols for various applications. It is the recommended therapeutic strategy to treat age-related macular degeneration and it represents a minimally invasive therapeutic approach for the treatment of certain types of cancer including skin, esophageal, head and neck, lung, and bladder cancers.[1,2] PDT causes its cytotoxic effects against harmful or unwanted cells or even pathogens based on the combined action of three elements: a photosensitizing agent, light and oxygen. More specifically, administration or application of the photosensitizer (PS) is followed by local irradiation of the pathological tissue area. Light exposure of the area occurs at the appropriate power, duration and most important wavelength. The latter, should be able to adequately penetrate the tissue in order to equally affect cells located at deeper tissue layers. Once the photosensitizer is appropriately light-excited in the presence of oxygen, a series of energy transfers and photochemical reactions is triggered, resulting in the production of singlet oxygen ($^1O_2$) and other highly reactive oxygen species (ROS).[1,3] These products initiate a domino of biochemical phenomena which can eventually cause significant toxicity and lead to cell death *via* apoptosis, necrosis or autophagy.[4,5] The advantages of PDT, such as high cure rates

[a]*Laboratory of Biomedical Optics and Applied Biophysics, School of Electrical and Computer Engineering, National Technical University of Athens, Zografou Campus, 15780 Athens, Greece. E-mail: ealexan@central.ntua.gr*
[b]*Laboratories of Structural Studies of Biomolecules and Pharmaceuticals with NMR, Institute of Biosciences and Applications, NCSR "Demokritos", Ag. Paraskevi, 153 10 Athens, Greece. E-mail: sagnou@bio.demokritos.gr*
[c]*Bioimaging and Cell analysis, Material and Chemical Characterisation Facility, University of Bath, Claverton Down, Bath BA2 7AY, UK*

with minimal toxicity in healthy tissues, specific targeting and selectivity, low side effects, potential use as an adjuvant therapy combined well with all other tumor interventions such as chemotherapy, surgery, radiotherapy or immunotherapy and finally its excellent cosmetic results, make it a very promising option in the treatment of cancer.[1,2]

An ideal photosensitizer should be able to address as many as possible of the following criteria: show strong absorption with a high extinction coefficient in the red/near infrared region of the electromagnetic spectrum (600–850 nm) to allow deeper tissue penetration; be an effective generator of singlet oxygen and other reactive oxygen species; exhibit favorable photophysical characteristics; have minimum dark toxicity; accumulate more in diseased/target tissue rather than the healthy cells; be a single, well-characterized compound, with a known and constant composition, stable in solution, serum or plasma with a simple and stable drug formulation; have an economical production route with feasible multi-gram scaling.[6]

Curcumin, the hydrophobic polyphenol found in the rhizome of turmeric (*Curcuma longa* L.), has been widely used in food coloring, drugs and cosmetics. A wide range of therapeutic properties and many exciting pharmacological effects have been reported for curcumin, including anti-inflammatory and antioxidant, chemopreventive and chemotherapeutic potential.[7,8] The photobiological and photokilling potential of curcumin and curcuminoids have been of great scientific interest since 1987,[9,10] investigating the mechanism of the photosensitization potential of such molecules.[9,11–15] Curcumin seems to adequately meet most of the prerequisites for a desirable, highly promising and "drugable" photosensitizer. It is biologically safe even at doses up to 12 g kg^{-1} day^{-1} and it can be produced affordably in gram-scale amounts with easy handling and storage requirements.[11,16] Many cancer cell lines *in vitro* show preferential uptake of a curcumin composite, in comparison to healthy cell lines.[17] Its photosensitisation mechanism is not yet fully known, but it has been observed to require oxygen.[9,10,18] Attention has been drawn on curcumin-derived photolytically produced species of active oxygen and more specifically singlet state oxygen, hydrogen peroxide and hydroxyl radicals.[10,18] Photobleaching experiments to a curcumin-based composite revealed a clear relationship between its degradation profile and the singlet oxygen production.[19] In terms of its photochemical properties, curcumin is characterized by a broad absorption spectrum between 300 and 500 nm with relatively high extinction coefficient. It can induce strong phototoxic reactions in micromolar concentrations.[20,21] As a result, curcumin appears as a promising photosensitizer in the treatment of local superficial infections and cancers. It would, therefore, be of great interest to investigate the photodynamic potential of curcumin derivatives characterized by higher absorption maximum and/or higher extinction coefficient anticipating that these characteristics will contribute to increased $^1O_2$ generation potential and hence photodynamic toxicity.[22]

The present work presents the results on the photophysical and photodynamic investigation of curcumin **1** and three synthetic curcumin derivatives, **2–4** (Fig. 1) as potential photosensitizers in cancer photodynamic therapy. Curcumin, compound **1**, is the primary curcuminoid in turmeric and all the commercially available extracts, accounting for at least 70% of the mixture, and it is the compound for which most studies have been reported predominantly using the commercial mixture and in very few cases as the pharmacologically pure compound. Bisdemethoxycurcumin, compound **2**, occurs also in the naturally extracted mixture but in a very small amount (approx. 2%). It is, therefore, important to evaluate the activities of the two individual curcuminoids separately, and not as part of the extracted mixture. Curcuminoid **3** is a curcumin derivative with no substitution on the aromatic ring and an additional double bond bilateral to the diketone moiety and, hence, extensive conjugation, while the *p*-dimethylamino substitution of **4** is anticipated to act as an electron donor to the aromatic ring and the conjugated diketone. The photophysical properties of the four curcuminoids such as absorption, fluorescence, photobleaching and free radical production have been investigated. Subsequently, their effect on cell viability in LNCaP prostate cancer cells, in the absence of light (dark toxicity) was evaluated. Moreover, the cell uptake and localization of the substances in LNCaP cells was monitored and their photodynamic efficiency was also evaluated. To the best of our knowledge, this is the first time that curcuminoids **3** and **4** are evaluated as potential PDT photosensitizers.

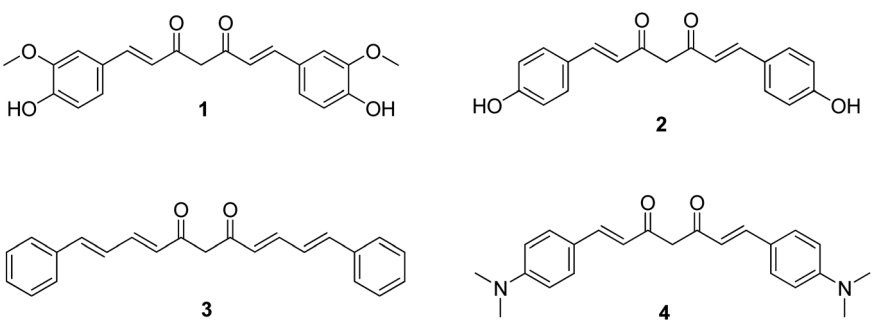

Fig. 1 Chemical structure of the curcuminoids investigated.

Materials and methods

Chemicals

Unless otherwise stated, all reagents and solvents were obtained from commercial sources and used without further purification. Air sensitive chemistries were performed in dry and inert conditions under an atmosphere of argon. All reactions were routinely checked by TLC on Silica gel Merck 60 F254 and compounds were purified by column chromatography on silica gel using the appropriate solvent systems or by preparative HPLC. The purity of the biological tested compounds was determined by analytical HPLC and was found to be greater than or equal to 95. The purity analysis was performed on a HPLC Shimadzu 2010EV (Column: Merck Purospher RP-C8, 250 × 4.6 mm, 5 μm particle size), equipped with a SPD-20A UV/Vis detector. Characterization of target compounds was established by a combination of ESI-MS and NMR spectrometry techniques. ^{1}H and ^{13}C NMR spectra were recorded on a Bruker Avance DRX spectrometer (500 MHz) at 25 °C. Chemical shifts are presented in ppm (δ) with internal TMS as standard. MS were obtained by the mass detector of the Shimadzu 2010EV HPLC system.

Stock solutions of curcuminoids **1–4** were freshly prepared by dissolving each powder in DMSO. Dulbecco's phosphate-buffered saline (DPBS), without $CaCl_2$ and $MgCl_2$, pH 7.4, dimethyl sulfoxide (DMSO) and 3-(4,5-dimethylthiazol-2-yl)-2,5-diphenyl-2*H*-tetrazolium bromide (MTT) were obtained from Sigma. RPMI 1640 medium was obtained from LGC Biomaterials. Fetal Bovine Serum, FBS, antibiotic–antimitotic and *t*-octylphenoxypolyethoxyethanol (Triton X-100) were purchased from Gibco.

Synthesis of curcumin derivatives[24]

All curcuminoids were synthesized in the lab to ensure the purity of the samples.

General procedure for synthesis of curcuminoids (1–4)

Acetylacetone (2.06 mL, 20 mmol) was added to a solution of boric anhydride (0.70 g, 10.0 mmol) and stirred at 80 °C for 0.5 h. To the reaction mixture the corresponding benzaldehyde (20 mmol) was added followed immediately by the addition of tributyl borate (21 mL, 80 mmol). The reaction mixture was stirred at 60 °C for 0.5 h. Subsequently, a solution of *n*-butylamine (0.8 mL, 10.0 mmol) was added dropwise over 30 min at 60 °C, and stirred overnight at 80 °C. Hydrochloric acid (1 N, 60 mL) was added, and the mixture was stirred for another 2 h at 60 °C. The organic layer was separated, and the aqueous phase was extracted with ethyl acetate (3 × 30 mL). The combined organic layers were washed with water, brine, dried over Na_2SO_4, filtered and concentrated under reduced pressure. The crude product was treated accordingly to afford the final curcuminoids as is described below.

1,7-Bis(4-hydroxy-3-methoxyphenyl)-1,6-heptadiene-3,5-dione (1, curcumin I). Acetylacetone reacted with vanillin according to the general method. The crude product was recrystallized in ethanol to afford the final product as yellow powder. Yield = 52%. ^{1}H NMR (500 MHz, DMSO-d_6) δ 7.54 (d, J = 15.3 Hz, 2H), 7.31 (s, 2H), 7.14 (d, J = 7.84 Hz, 2H), 6.81 (d, J = 8.0 Hz, 2H), 6.74 (d, J = 15.8 Hz, 2H), 6.06 (s, 2H), 3.83 (s, 6H). ^{13}C NMR (500 MHz, DMSO-d_6) δ 183.1, 149.4, 147.9, 140.7, 130.3, 126.3, 123.1, 121.0, 115.7, 111.3, 100.8, 55.7. MS (m/z) $[M + H]^+$ calc. for $[C_{21}H_{21}O_6]^+$ 369.13, found: 369.25.

1,7-Bis(4-hydroxyphenyl)-1,6-heptadiene-3,5-dione (2, curcumin III). Acetylacetone reacted with 4-hydroxybenzaldehyde according to the general method. The crude product was recrystallized in ethanol to afford the final product as yellow powder. Yield = 34%. ^{1}H NMR (500 MHz, DMSO-d_6) δ 7.57 (d, J = 8.1 Hz, 4H), 7.55 (d, J = 15 Hz, 2H), 6.82 (d, J = 8.3 Hz, 4H), 6.67 (d, J = 15.9 Hz, 2H), 6.04 (s, 1H). ^{13}C NMR (500 MHz, DMSO-d_6) δ 183.7, 160.3, 140.8, 130.8, 126.3, 121.3, 116.4, 101.4. MS (m/z) $[M + H]^+$, for $[C_{19}H_{17}O_4]^+$ 309.11. Found: 309.10.

(1*E*,3*E*,8*E*,10*E*)-1,11-Diphenylundeca-1,3,8,10-tetraene-5,7-dione (3). Acetylacetone was reacted with cinnamaldehyde according to the general method. The crude product was recrystallized by dichloromethane/hexane to afford the final product as yellow powder. Yield = 63%. ^{1}H NMR (500 MHz, DMSO-d_6) δ 7.59 (d, J = 7.4 Hz, 4H), 7.50–7.30 (m, 8H), 7.23–7.07 (m, 4H), 6.38 (d, J = 15.1 Hz, 2H), 6.09 (s, 2H). ^{13}C NMR (500 MHz, DMSO-d_6) δ 182.93, 141.06, 140.39, 136.13, 129.11, 128.92, 127.77, 127.38, 127.29, 101.39. ESI-MS (m/z) $[M + H]^+$ calc. $[C_{23}H_{21}O_2^+]$ 329.15, found 328.70.

(1*E*,6*E*)-1,7-Bis(4-(dimethylamino)phenyl)hepta-1,6-diene-3,5-dione (4). Acetylacetone reacted with 4-dimethylamine benzaldehyde according to the general method. The crude product was recrystallized by dichloromethane/hexane to afford the final product as deep red powder. Yield = 42%. ^{1}H NMR (500 MHz, DMSO-d_6) δ 7.62–7.41 (m, 6H), 6.74 (d, J = 8.5 Hz, 4H), 6.59 (d, J = 15.3 Hz, 2H), 5.97 (s, 2H), 2.99 (s, 12H). ^{13}C NMR (500 MHz, DMSO-d_6) δ 182.89, 151.63, 140.48, 134.60, 131.03, 128.92, 122.15, 118.62, 111.88, 100.39, 39.35. ESI-MS (m/z) $[M + H]^+$ calc. for $[C_{23}H_{27}N_2O_2^+]$ 363.21, found 363.15.

Spectroscopic methods

Absorption. UV-Vis absorption spectra were recorded using 4.5 ml volume cuvettes in the PerkinElmer Lambda 35 UV/VIS Spectrometer. The wavelength range was 300–700 nm and the scan speed was set at 480 nm min^{-1}. The absorbance of each curcuminoid in DMSO (3 ml samples) was measured at a final concentration of 20 μM, 10 μM, 5 μM, 1 μM and 0.5 μM. The measurements were performed in triplicates for each concentration point. Moreover, the absorbance of curcuminoids at 10 μM concentration was recorded in various solvents, namely DMSO, ethanol and PBS.

All absorption measurements were carried out at room temperature. The samples were freshly prepared just before measurements.

Fluorescence. Fluorescence spectra were obtained in DMSO solutions (0.3 μM and 0.5 μM) using 4.5 ml volume cuvettes in the PerkinElmer LS 45 Luminescence Spectrometer. Each curcumin derivative sample (3 mL) was excited at the wavelength

that corresponds to its maximum absorption, *i.e.* 435 nm for **1** and **3**, 425 nm for **2** and 497 nm for **4**. The slit width was set at 10 nm both for excitation and emission. Scan speed was adjusted to 480 nm min^{-1}.

All fluorescence measurements were carried out at room temperature. The samples were freshly prepared just before measurements.

Irradiation device

Irradiation was performed using a custom-made illumination device developed in the Laboratory of Biomedical Optics and Applied Biophysics, National Technical University of Athens. It consisted of a Bridgelux Power LED 10 W light source, emitting at 430 ± 10 nm, coupled to special optics in order to provide uniform, circular illumination. The device was also equipped with a potentiometer in order to adjust power output and a cooling base with a build-in fan. Irradiation power was assessed using a power meter.

Photobleaching

Each curcuminoid sample (0.5 μM for **1** and **4**, 0.2 μM for **2** and **3**) was irradiated at 12.5 mW cm^{-2}. Fluorescence spectra were acquired every 1 min between 0–10 min and every 5 min between 10–30 min. The fluorescence emission maximum was then recorded in order to evaluate photobleaching.

ROS production

Nicotinamide Adenine Dinucleotide (NADH), a pyridine nucleotide and biologically active form of nicotinic acid, is a coenzyme necessary for the catalytic reaction of certain enzymes that absorbs at 340 nm. Following the decrease in absorbance at 340 nm, NADH consumption and its conversion to NAD^+ was assessed and hence the existence of free radicals in the solution.

Freshly prepared solutions consisting of 10 μM of each curcumin derivative, 100 μM NADH and 0.1 mM EDTA, were irradiated at 4.70 mW cm^{-2} for 20 min. Every 1 min, samples were returned to the spectrometer and the absorption spectra were acquired. The absorption peak at 340 nm was recorded.

Cell culture conditions

The human prostate cancer cell line LNCaP was obtained from the American Type Culture Collection (ATCC). The cells were cultivated in 75 cm^2 culture flasks (Corning) in RPMI-1640 medium supplemented with 10% heat inactivated Fetal Bovine Serum, FBS, and 0.1% antibiotic–antimitotic. Cells were kept at 37 °C in a 5% CO_2 humidified incubator, trypsinized and re-seeded into fresh medium every 3–5 days.

Intracellular localization

LNCaP cells 10×10^5 were seeded on Nunc™ glass base dishes (ThermoFisher Scientific, Rochester, NY, USA) and incubated overnight in 2 mL of DMEM complete medium in the same conditions as previously described. Cells were subsequently treated with curcuminoids (3 μM final concentration) for 1 h. Specimens were examined on a Leica TCS SP8 MP (Wetzlar, Germany) multiphoton confocal microscope equipped with an Argon laser (excitation lines at 458, 476, 488, 496 and 514 nm), a DPSS 561 laser (excitation line at 561 nm) and an IR MaiTai DeepSee Ti:Sapphire laser (Spectra-Physics, Santa Clara, CA, USA) for multiphoton applications.[23] Images were acquired with the LAS X software (Leica Microsystems CMS GmbH, Wetzlar, Germany) and are presented without any post-processing.

Cell viability evaluation

Cell viability was assessed by the MTT [3-(4,5-dimethylthiazol-2-yl)-2,5-diphenyl-2*H*-tetrazolium bromide; Sigma] colorimetric assay, which measures the capacity of mitochondrial dehydrogenase to reduce MTT to purple formazan crystals. The MTT test assesses the number of surviving cells.

The calibration curve of the LNCaP cells absorbance was made prior to the experiments. 24 h after photodynamic treatment, the medium was removed and the MTT solution was added to each dish. The cells were kept in the humidified incubator for 3 h to allow metabolism of MTT. After incubation, the formazan crystals were solubilized by adding the MTT solvent (10% Triton X and 0.1 N HCl in isopropanol). Absorbance was measured using a computer controlled PerkinElmer Lambda 35 UV/VIS Spectrometer. Spectra were collected for a wavelength range between 380 and 700 nm. All measurements were carried in triplicate and data were expressed as mean ± standard deviation. From each spectrum, the absorbance at 690 nm was subtracted (as noise) from the absorbance at 565 nm (maximum peak of formazan absorption spectrum). From these values of absorption and the calibration curve, cell viability percentages of treated and control samples were calculated.

Dark cytotoxicity

For determination of dark cytotoxicity, LNCaP cells were incubated for 24 h in the dark at a concentration range of 1 μM, 3 μM and 5 μM of each derivative. When the incubation time was completed, the cells were washed with 1 mL DPBS, followed by addition of fresh medium and incubation for 24 h. Cellular viability was measured with the MTT viability test. All measurements were carried out in triplicate. All data were expressed as mean ± standard deviation.

Light cytotoxicity

For determination of light dependent cytotoxicity, cells were irradiated with 3 mW cm^{-2}, 6 mW cm^{-2} and 9 mW cm^{-2}. The exposure time was 60 s. Irradiation occurred in the presence of 300 μL DPBS for each Petri dish. Fresh medium was added when the irradiation was completed. 24 h post irradiation, cellular survival was measured with the MTT assay. All measurements were carried out in triplicate and data were expressed as mean ± standard deviation.

Photodynamic treatment

Cells were incubated with 3 μM freshly prepared solution of each curcuminoid in enriched medium for 1 h. Before light

exposure, the culture medium containing the photosensitizers was removed from the dishes and PBS was added (300 μL) until the cell monolayer was slightly covered. Irradiation was performed at room temperature with the 430 nm LED-based illumination device. Irradiance was adjusted to 6 mW cm^{-2} and the exposure times were 60 s, 120 s and 180 s yielding 360, 720 and 1080 mJ cm^{-2} fluence rates, respectively. Following irradiation, fresh medium was added and the cells were maintained in the humidified incubator for 24 h. Finally, cellular survival was measured with the MTT assay. All measurements were carried out in triplicate. All data were expressed as means ± standard deviation.

Results

The desired symmetrical curcuminoids **1–4** were successfully synthesized according to the literature with slight modifications.[24] The reaction of boric anhydride with acetylacetone is initially employed to form an acetone-boric oxide complex aiming to eliminate the reactivity of the central methylene group towards Knovenagel condensation. In this way, aldol condensation takes place in the presence of tributyl borate as a desiccant, between the corresponding benzaldehyde and the side methyl methyl moieties, instead of the more reactive central methylene group. The final treatment with 1 N hydrochloric acid released the β-diketone moiety from the borate complex to afford the desired product.

Photophysical properties

Absorption spectra. The absorption spectra of curcuminoids **1–4** in DMSO are shown in Fig. 2. Three of them, **1–3**, show similar spectral characteristics with a peak at around 430 nm, whereas compound **4** exhibits according to our design, a significant and desirable red shift with an absorption peak at 497 nm.

Table 1 summarises the wavelengths of maximum absorption and the extinction coefficient for the four curcuminoids

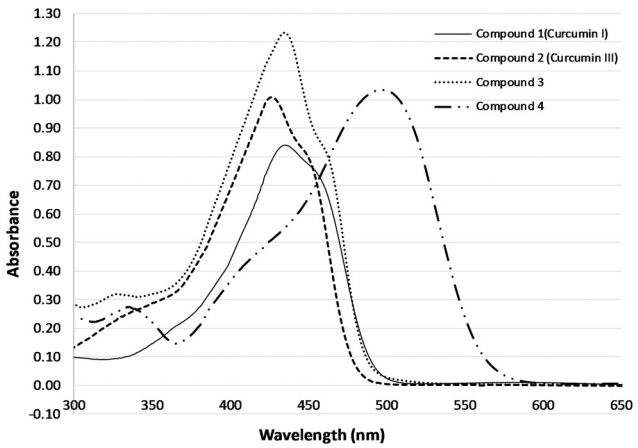

Fig. 2 Absorption spectra of curcuminoids **1** (curcumin I), **2** (curcumin III), **3**, **4** in DMSO (20 μM final concentration).

Table 1 Wavelength of maximum absorption and extinction coefficient (±SD) for the four synthetic derivatives of curcumin, at concentration 20 μM in DMSO

Curcumins	λ_{max} (nm)	ε (cm^{-1} M^{-1})
1 (curcumin I)	435	42 200 ± 14
2 (curcumin III)	426	50 180 ± 21
3	435	61 300 ± 13
4 (di-NCH_3 curcumin)	497	51 700 ± 39

investigated herein. Curcumin I exhibited the lowest extinction coefficient of 4.2×10^4 cm^{-1} M^{-1} whereas derivative **3** was found to have the highest extinction coefficient of 6.1×10^4 cm^{-1} M^{-1}. Compounds **2** and **4** showed comparable extinction coefficients of a value around 5×10^4 cm^{-1} M^{-1}.

The absorption spectra of the four curcuminoids (10 μM) in different solvents, DMSO, ethanol (EtOH) and PBS are depicted in Fig. 3. When organic solvents were used such as DMSO or ethanol, the compounds present the characteristic absorption spectrum. DMSO is considered as a hydrogen acceptor solvent whereas alcohols can act as either hydrogen donors or acceptors depending on the molecular structure of the solute. There was no significant shift or any other alteration in the absorption spectrum of four derivatives when changing from DMSO to ethanol solutions, despite the difference in polarity.

In the case of water-based solution such as PBS, which was used as a biologically relevant solvent, there is a significant decrease in absorption and a shift in the wavelength of maximum absorption to lower wavelengths, which may be related to the tendency of curcuminoids to form aggregates in aqueous media.

Fluorescence spectra. The fluorescence spectra of the four curcumin derivatives in DMSO are presented in Fig. 4. Compounds **1–3** exhibit similar fluorescence emission maxima, whereas curcuminoid **4** fluoresces at longer wavelengths, as expected based on its higher excitation wavelength. Compound **2** exhibits the strongest fluorescence emission, as it was necessary to reduce its concentration to 0.3 μM, to acquire an emission signal of comparable intensity to the rest of the compounds for which emission was recorded at a concentration of 0.5 μM whereas **1**, showed the weakest fluorescence emission.

Fluorescence emission maximum presented a linear relationship with concentration, in the range of 0.01 μM to 0.5 μM, for all the tested substances (data not shown).

Photobleaching by measuring absorbance and fluorescence

Changes in both absorbance and fluorescence emission maximum of the four curcumin derivatives, relative to the time of illumination, were monitored. In Fig. 5, changes in fluorescence intensity as percentage of the initial fluorescence before irradiation were presented.

In the case of **4**, the drop in fluorescence emission maximum is approached linearly in relation to irradiation time, while in all other cases there is an exponential decrease.

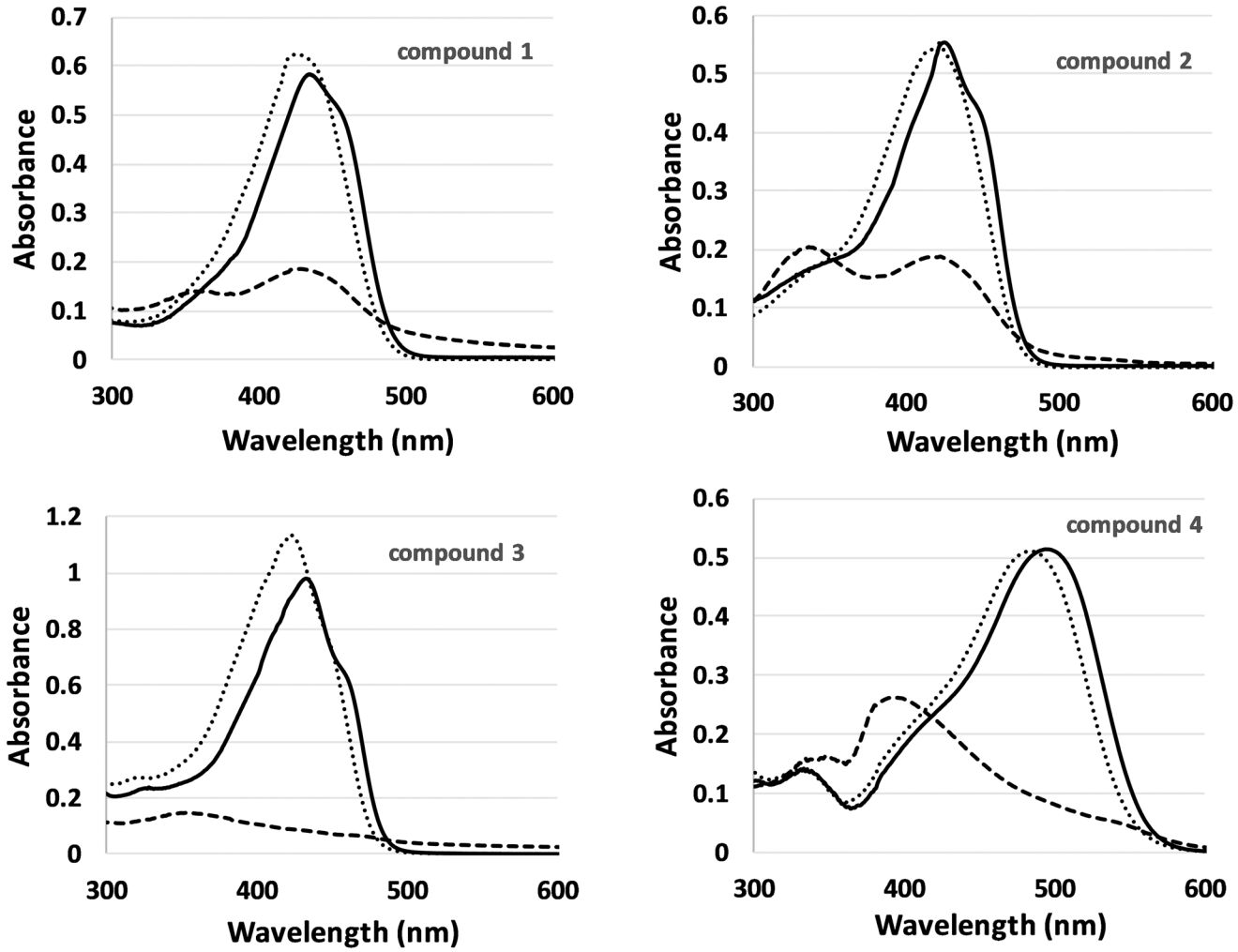

Fig. 3 Absorption spectra of the four curcumin derivatives (10 μM) in different solvents: DMSO (solid line), ethanol (dots) and PBS (dashes).

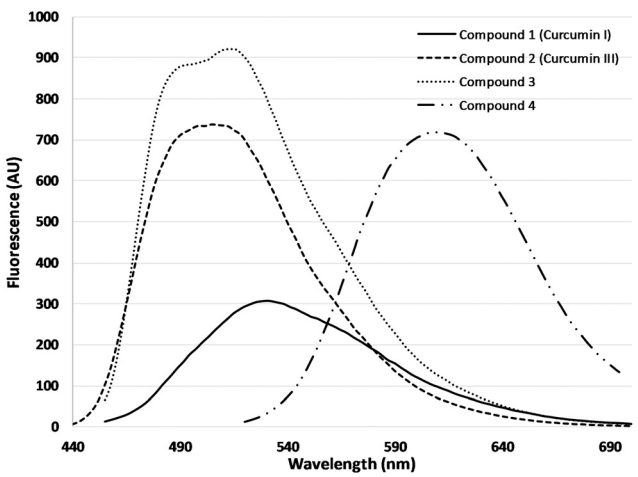

Fig. 4 Fluorescence spectra of curcuminoids, **1** (0.5 μM, λ_{exc} = 435 nm), **2** (0.3 μM, λ_{exc} = 425 nm), **3** (0.5 μM, λ_{exc} = 435 nm), **4** (0.5 μM, λ_{exc} = 497 nm) in DMSO.

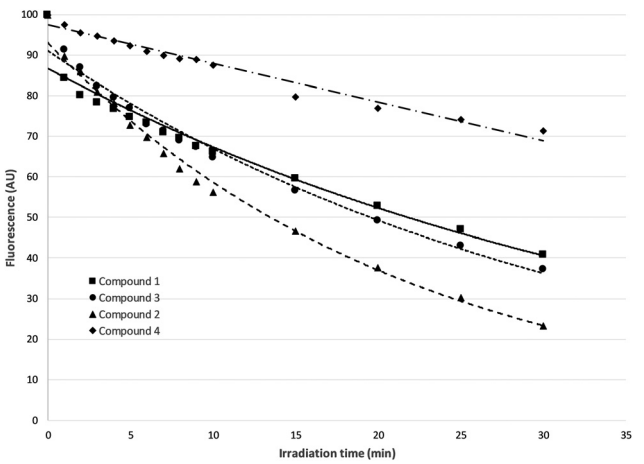

Fig. 5 Fluorescence emission maximum intensity changes as a function of illumination time for the four curcuminoids solutions in DMSO at concentrations of 0.5 μM for compounds **1** and **4** or 0.2 μM for compounds **2** and **3**, after irradiation at 12.5 mW cm^{-2}.

As it can be seen, derivative **4** is characterized by a significant resistance to photobleaching, compared to the other three derivatives, making it the most photostable of the four curcumin derivatives that were examined. The highest photobleaching was observed for compound **2** (curcumin III).

Absorption values were reduced in a similar way with illumination time (data not shown).

Production of free radicals

The relationship between the absorption peak of NADH at 340 nm and the time of irradiation is represented in Fig. 6. The drop in the absorption peak at 340 nm, is indicative of the formation of the oxidized NAD^+, resulting from the production of reactive oxygen species (ROS).

In case of derivative **4**, the drop of the absorption peak is linear. For curcuminoids **2** and **3**, the reduction is logarithmically approached, whereas **1** presents an exponential decrease with irradiation time.

It is obvious from the graph, that Compounds **2** and **3** produce the largest amount of free radicals with very short irradiation times, a result considered positive for potential photosensitizers.

Dark cytotoxicity

The results on LNCaP cell viability after incubation in the dark with curcumin derivatives at concentrations of 1 μM, 3 μM, 5 μM, are shown in Fig. 7. Cellular viability was evaluated by means of the MTT assay 24 h post incubation with the potential photosensitizers.

Cell viability was not significantly affected upon incubation in the dark at 1 μM and 3 μM concentrations of the test compounds in a statistically significant manner. Incubation with 5 μM concentration of the photosensitizers, however, caused a considerable decrease in cell survival. Consequently, the photodynamic treatment experiments were performed using 3 μM of the curcuminoid concentration.

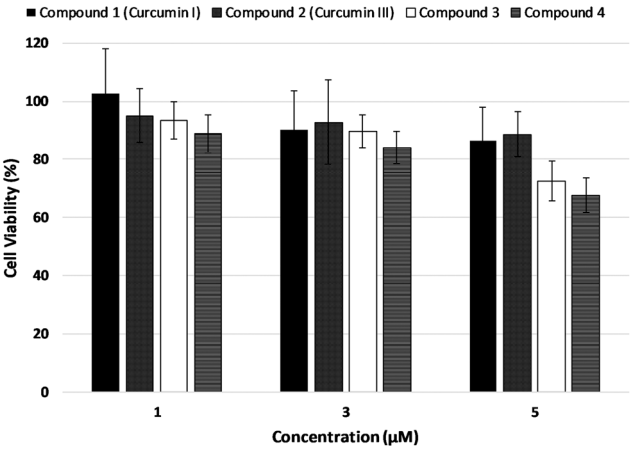

Fig. 7 Dark toxicity results of the four derivatives at various concentrations (1, 3 and 5 μM) in LNCaP cells. After 24 h treatment with each compound, the cells were incubated in growth medium for another 24 h period. The data are expressed as mean of three experiments. Error bars present standard deviation.

Light cytotoxicity

Light dependent cytotoxicity, in the absence of any test compound, is presented in Fig. 8. Irradiance of 3 mW cm^{-2}, for 60 s irradiation time, not only is not toxic to the cells, but also caused a slight increase in cell viability compared to non-irradiated cells. On the contrary, when irradiance of 9 mW cm^{-2} was used, there was a 25% decrease in cellular viability.

For irradiance of 6 mW cm^{-2}, there was no significant effect on cell survival, and consequently this irradiance value was used in the photodynamic treatment experiments.

Intracellular localization

Intracellular localization of the four curcumins was studied using confocal fluorescence microscopy. Fig. 9 includes indica-

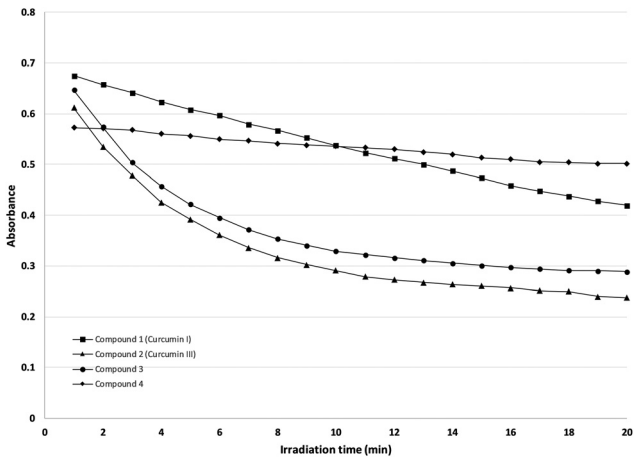

Fig. 6 The variation of the absorbance peak of NADH at 340 nm in relationship with time of irradiation. The diagrams refer to solutions of each derivative at concentration of 10 μM in DMSO. Each solution contains 100 μM NADH and 0.1 mM EDTA.

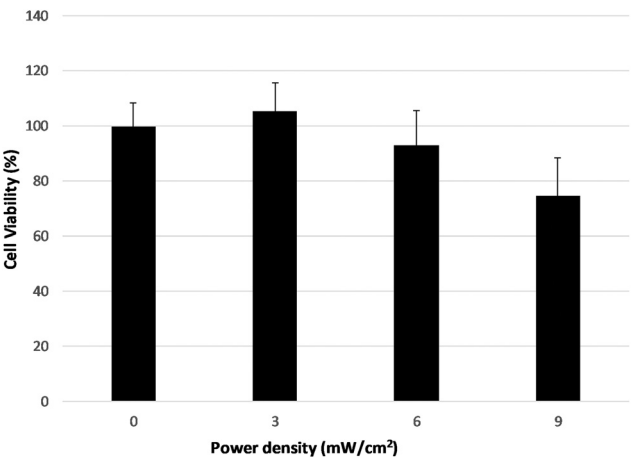

Fig. 8 Light-induced cell cytotoxicity in LNCaP cells, without any photosensitiser, after irradiation for 60 s with irradiance set to 3 mW cm^{-2}, 6 mW cm^{-2} and 9 mW cm^{-2}.

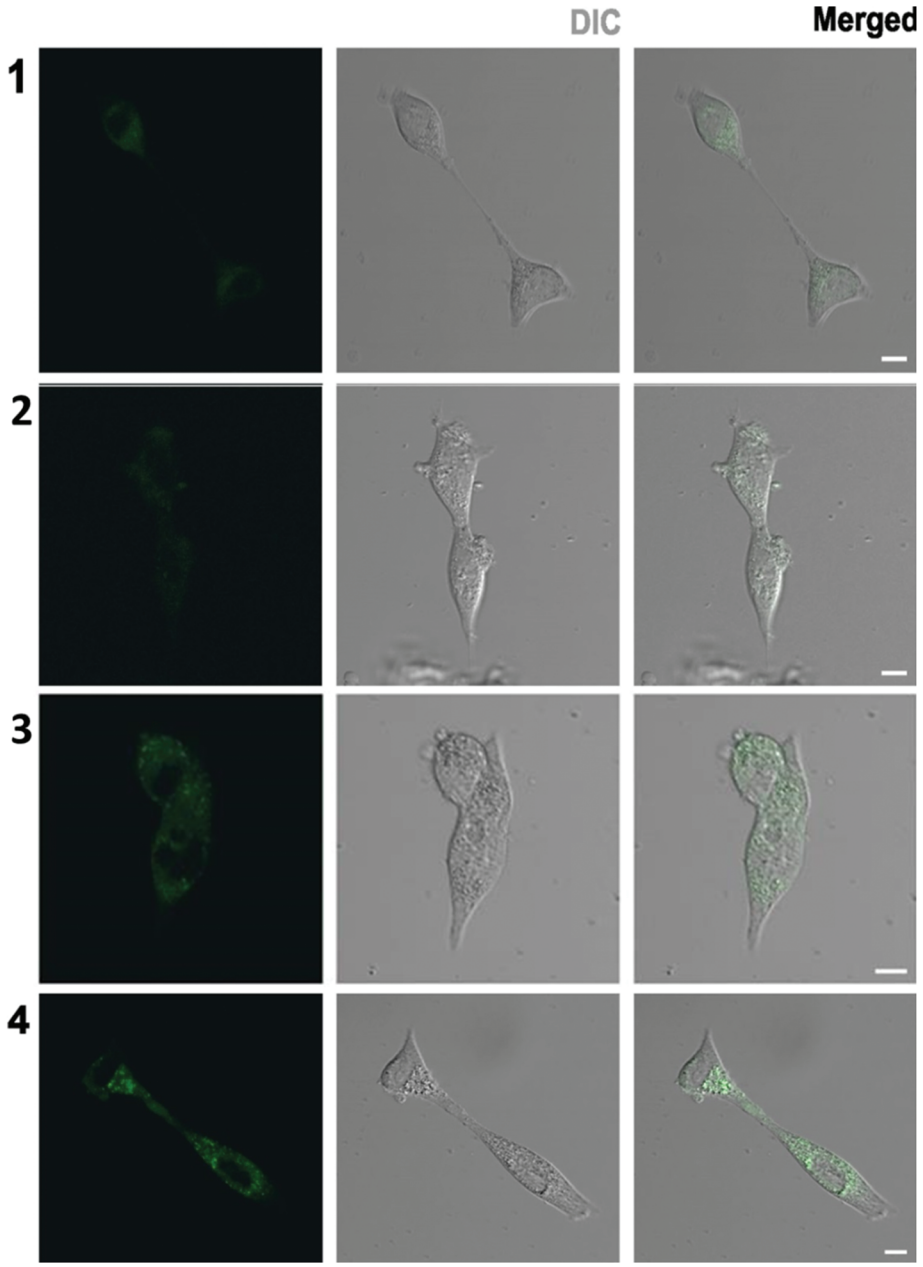

Fig. 9 Confocal fluorescence microscopy on live LNCaP cells incubated for one hour with 3 μM of each curcumin derivative; left column: images acquired with confocal microscope – for compounds **1** and **2** λ_{ex} = 458 nm whereas for compounds **3** and **4** λ_{ex} = 488 nm; middle column: brightfield images of the cells; right column: merged brightfield and confocal images.

tive images of LNCaP cells incubated with 3 μM of each synthetic curcumin derivative for one hour. Bright field images showing the cell morphology are presented in the middle column, whereas the corresponding fluorescence images are shown on the left. On the right column, merged images of optical and confocal mode are displayed.

Upon 1 h incubation with 3 μM of the compounds, fluorescence images of the cells revealed that photosensitizers have entered the cells sufficiently. The lowest cellular fluorescence intensity was observed upon treatment with **1**, curcumin I, whereas cellular incubation with compound **2** resulted in significantly more intense fluorescence imaging of the cells. Finally, the cell fluorescence uptake observed after treatment with **3** and **4** was of the highest intensity.

Fluorescence images showed that none of the substances affected the cell structure. There was no nuclear localization exhibited by any of the test compounds. However, some perinuclear accumulation could be noticed. Furthermore, this cytoplasmic or perinuclear localization did not seem to be evenly distributed and some more intensely fluorescent spots could be identified.

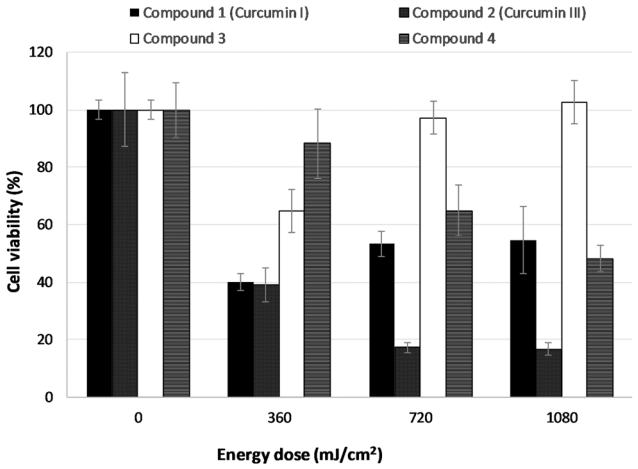

Fig. 10 The photodynamic efficiency of the four synthetic curcuminoids on LNCaP cells 24 h post irradiation at 451 nm. The initial photosensitizer concentration was 3 μM and the cells were treated for 1 h prior to photoactivation.

Photodynamic treatment

LNCaP cells were incubated with 3 μM of each of the four curcuminoids for one hour. Subsequently, the cells were irradiated and the induced phototoxicity was assessed 24 h post PDT by the MTT assay. Fig. 10 presents the results obtained for the effect of the test photosensitizers on cell viability for various irradiation times and consequently various irradiation energy doses.

Compounds **2** and **4** exhibited a dose-dependent decrease in cell survival. In the case of curcuminoid **2** even at the lowest energy dose (360 mJ cm^{-2}) 40–50% of the cell population was killed 24 h post irradiation whereas, with compound **4**, the LD_{50} value was achieved at the highest energy dose of 1080 mJ cm^{-2}. On the other hand, compounds **1** and **3** caused an initial cell-killing effect at low doses, which seemed to be reversed at higher energy irradiation doses. It is worth noting that compounds **1** and **2** had a detrimental effect on cell viability even at the lowest energy dose of 360 mJ cm^{-2}.

Discussion

Curcumin as a photosensitizing agent for PDT has been the subject of a number of studies either in antimicrobial PDT[25] or against various human cancer cells.[13,26–28] Some of the limitations reported for the potential clinical application of curcumin in PDT are its poor solubility, stability and photostability in aqueous solutions as well as the rapid metabolism and systemic elimination.[29–33] In most studies, commercially available curcumin is used. In this study pure samples of curcumin (**1**) synthesized in the lab are employed in the study of the PDT related properties. Furthermore, to the best of our knowledge, there is no study for PDT with curcumin itself or any curcuminoids on human prostate cancer cells. Moreover, in this study curcumin **1**, was comparatively evaluated in terms of physicochemical stability and photodynamic potential to the natural curcumin, **2**, which lacks the two methoxy groups at the *meta*-position to the hydroxyl moiety of **1**, as well as two newly synthesized curcuminoids. Compound **3**, had no substitution on the aromatic ring but possessed an extra double bond between the aromatic ring and the β-diketone which was anticipated to increase electron delocalization. Finally, curcuminoid **4** was designed to possess the dimethylamine- to replace the *para*-phenolic groups of **2**, as potential electron donor moieties.

Indeed, all curcumin derivatives at different concentrations maintained a characteristic absorption spectrum for the whole range of concentrations that were used and the absorbance intensity changed linearly relative to the concentration in all cases in accordance with results reported from similar studies.[18,34–36] Compounds **1**, **2**, and **3** exhibited significant absorption between 350 and 480 nm, whereas **4** was red shifted absorbing between 400 and 550 nm. This had been anticipated according to the design of the molecule, based on the electron donor character of the dimethylamino- group at the *para*-position to the unsaturated chain. Bearing in mind that longer excitation absorption corresponds to deeper tissue penetration, compound **4** exhibits a favorable and advantageous property for PS applications.

In addition, all curcuminoids tested showed relatively high extinction coefficient (ε) in the wavelength of their maximum absorbance (Table 1), ranging from 42 200 to 61 300 M^{-1} cm^{-1} compared to some of the clinically tested photosensitizers such as Photofrin® (~3000 M^{-1} cm^{-1} at 632 nm), PPIX (~5000 M^{-1} cm^{-1} at 632 nm) and m-THPC (~35 000 M^{-1} cm^{-1} at 652 nm). Molecules with a high extinction coefficient (ε) are more desirable as PS since they may require a smaller amount to be administered to the cells and cause significant damage upon light activation without any undesirable side effects which may occur due to excessive PS dosage.[37,38] The curcuminoids scaffold seems to be a privileged structure in that respect. It is worth mentioning that the additional double bond of **3** seemed to favor even further the high extinction coefficient profile of the compounds, exhibiting the highest ε of all four molecules. Our results are in good agreement with previous reports[39] which investigated and related the physicochemical and photochemical properties of curcuminoids with the keto–enol tautomeric form as well as the substitution pattern of the aromatic ring. In the case of **3** the absence of any hydroxyl- or amino-groups and the addition of a double bond increases the hydrophobicity of the molecule and minimizes the solvent interactions. In the case of the polar organic solvents, it is the keto–enol equilibrium, which provides a sufficient center of solvent–molecule interactions. Curcuminoids **1** and **2** possess a phenolic OH– group and in the case of **4** the nitrogen containing aromatic substitution may all form intramolecular H-bonds and π-stacking interactions leading to the formation of aggregates when dissolved in aqueous media.[31–33,40,41] The increased hydrophobicity, poor water solubility which easily leads to aggregated species

under physiological conditions and drastically lowers the quantum yields of ROS production, has long been one of the main limitations for the clinical use of PDT. To this end, the use of transporters like proteins, liposomes or nanoparticles has been exploited to protect curcumin and other photosensitizers against the undesirable solvent effects.[33] This proved to be beneficial to PDT applications. This presents a very interesting future prospect of this study to enhance the properties of these four curcuminoids and elucidate further their mechanism of action.

In terms of their fluorescence emission and in accordance to previous reports[12,42] curcumin I (**1**) and (**2**) exhibit different fluorescent properties which may be ascribed to either the difference in H-bond acceptor/donor properties of the phenolic OH, or the difference in strength of the intramolecular H-bond in the keto–enol moiety due to the lack of methoxy group. All four curcumin derivatives displayed intense fluorescence emission and as a result they can be used not only in the application of photodynamic therapy, but also in photodynamic diagnosis. Especially, compound **4** presented a red shift in both absorption and fluorescence properties, with emission maximum at 610 nm upon excitation at 497 nm. Based on these characteristics, compound **4** can be utilized as a theranostic agent not only for superficial but also for in depth lesions.

In photobleaching experiments, the fluorescence emission maximum exhibited an exponential decay with respect to irradiation time in the cases of curcuminoids **1**, **2** and **3** in DMSO solutions. Photobleaching of compound **3** has been shown to proceed faster than **1** in DMSO, in agreement to our results, and we have similarly identified that **2** undergoes a comparable photodegradation rate with **3**. On the contrary, in the case of compound **4**, the most photostable photosensitizer, the fluorescence decay was approximated linearly and the substance was characterized by resistance to photobleaching. Even though in terms of photostability, curcumin meets the standards for a promising PS, however, a reasonable balance should exist between acute and prolonged photosensitivity and post-treatment random excitation of the photosensitizer.

Absorption was reduced in a similar way with illumination time (data not shown), indicating that the decrease is definitely due to a lower extinction and maybe due to a lower fluorescence yield. The observed findings suggest that it is not photomodification but true photobleaching. In photomodification, the original absorption spectrum diminishes and new absorption peaks are emerged. In the case of all the compounds studied in the current paper, there were no new peaks observed in the absorption spectra only reduced absorption in the same wavelengths.[43]

Another important characteristic of an ideal photosensitizer is its ability to produce Reactive Oxygen Species (ROS). Upon irradiation, the photosensitizer transforms from its ground singlet state to a short-lived excited singlet state of higher energy which eventually may be converted to a relatively long-lived excited triplet state *via* intersystem crossing.[1] Compounds **2** and **3** exhibited the highest ability to produce free radicals, after irradiation at 430 nm, which is close to the max absorption and corresponds to increased molecular excitation. Curcumin **1** produced less free radicals and the corresponding drop in absorption was approached linearly, indicating a slower rate of ROS production. Finally, **4** revealed a rather small ROS production ability compared to the other three derivatives. It should be noted, however, that the irradiation at 430 nm is not sufficiently high to excite the molecules since the absorption maximum of this compound was shifted to almost 500 nm. From a structural point of view, it is evident that the lack of the methoxy-aromatic substitution in **2** and the additional conjugated double bond also with the completely unsubstituted aromatic moiety in **3** favors both photodegradation and free radical production.

One of the great advantages of the potential clinical application of curcumin is the fact that being a natural product it is safe to use even at high daily doses. In accordance, all four compounds were found non-toxic against the LNCaP cell line after a 24 h treatment in the dark, when tested at concentrations up to 10 μM. There is one literature evidence suggesting that even at concentration of 20 μM of compound **1** and 48 h treatment the cell viability of LNCaP was reduced only by 30%.[44] This low dark toxicity of the compounds provides the necessary degree of selectivity to their photodynamic application since light activation is a prerequisite for their cytotoxic action and cell killing effect.

Our light-induced cytotoxicity experiments demonstrated the importance of performing light-only experiments for every cell line used in a study. At an irradiance of 3 mW cm^{-2} and 6 mW cm^{-2} for 60 s no or little light toxicity was observed. On the contrary, previous studies of our group, with the same cell line irradiated with 6 mW cm^{-2} at a different wavelength significantly reduced cell viability.[45] This finding implies the presence of a wavelength dependence of cell line light toxicity regardless of the irradiation power.

In light activation experiments all four curcuminoids exhibited cytotoxicity after irradiation. In particular, compounds **1**, **2** and **3** caused at the lowest fluence tested a very significant reduction in LNCaP cell survival while the reduction in cell population was less for curcuminoid **4**. This acute light-induced toxicity may be related to their effective radical production which was clearly demonstrated in our study. Curcumin, **1**, has been previously reported to exhibit such a PDT energy dose dependence. Micromolar concentrations (in the range of 0.4–13.5 μM) of the photosensitizer, in combination with low light, were shown to be effective for the treatment of oral cancers, after 3 h of incubation.[13] Furthermore, a significant reduction of hepatoblastoma (HuH6, HepT1) and hepatocellular carcinoma (HepG2, HC-AFW1) cell viability was observed, after their treatment with curcumin **1** and exposure to blue light. It was derived that curcumin mediated PDT effectively enhanced the anti-tumor properties in epithelial liver cancer cells by inducing loss of viability *via* ROS production.[46]

Upon increasing light fluence, however, two distinct profiles were observed regarding their photodynamic effect on LNCaP cells. More specifically, compounds **2** and **4** presented an increasing PDT efficacy with increasing energy dose resulting in increased cytotoxicity effects. Compounds **1** and **3** exhibited an inverse dose–response with the lowest fluence rate used (360 mJ cm^{-2}) causing the most powerful PDT effect, whereas higher fluence rates resulted in significantly less cytotoxic effect in a dose-dependent manner. It may be suggested that at higher fluence rates, increased radical concentration may favour radical quenching through intermolecular interactions resulting in formation of non-active adducts before the PD effect may be exerted, or implies fast degradation of cellularly incorporated curcumin.[47,48] Tanaka, Hamblin *et al.* observed a similar behavior when they examined the effect of Photofrin-mediated photodynamic therapy on bacterial arthritis in mouse model.[49,50] After application of PDT for the treatment of an MRSA arthritis infection in the mouse knee (1 μg Photofrin, 635 nm diode laser illumination), a biphasic light dose response occurred. The greatest reduction of MRSA CFU was seen with a fluence of 20 J cm^{-2}, whereas lower antibacterial efficacy was observed with fluences that were lower but also higher.[49,50]

A very rapid and very effective PDT action that is reversed upon longer irradiation time constitutes an exciting property, which is able to address the limitations of prolonged photosensitivity, a usual PDT drawback.

Taking advantage of their intense fluorescence properties, their cellular localization and concentration was studied by means of confocal microscopy. Although, the fluorescence intensity of the photosensitizer inside the cells depends on both its intracellular concentration and its fluorescence quantum yield, it can be considered as a meter of its bioavailability. Intracellular localization of the photosensitizer is of primary importance as the produced ROS are characterized by very short lifetimes and their targets should be very close to their production site.[51–53] Therefore the subcellular localization of the photosensitizer essentially determines the localization of the primary targets. There was no specific cellular localization observed for curcumin **1** in LNCaP cells, contrasting previous findings where mitochondrial curcumin localization was reported in non-small-cell lung cancer A549 cells, and membrane preference was observed in MCF7 breast cancer cells.[54,55] However, it is important to note that higher (10 or 20 μM) curcumin concentrations and longer incubation times up to 4 h[54,55] and 24 h (ref. 56 and 57) were employed in those studies, that may have indeed promoted the observed cellular localization.

On the other hand, curcuminoids **2**, **3** and **4** indeed accumulated intracellularly in specific areas of the cells, which did not colocalised with Mitotracker or Lysotracker staining, suggesting that they do not localize in mitochondria or lysosomes (data not shown). The apparent cellular localization of **2** and **4** may be associated with their PD effect in LNCaP cells. Especially, in the case of **4**, where a relatively small amount of ROS was observed, this intense cellular influx and accumulation may be responsible for the observed light energy dose dependent PD effect. Additionally, the intracellular localization of curcuminoid **2**, may have been the reason for a more dramatic PD effect against LNCaP cells, since the high ROS production capacity of **2** was also accompanied by this special accumulation inside the cell, causing possibly more cellular damage.

In conclusion, the four curcuminoids presented promising characteristics in terms of PDT efficacy. Pure, synthetically produced materials were used, even for the naturally occurring curcumins **1** and **2**, making the correlation of structure to activity direct. All of them showed sufficient ROS production and remarkably short LD_{50}, especially compound **2**, making them highly promising photosensitizers. It is the first time that these four curcuminoids are tested against this cell line. Curcuminoid **4** achieved a significant red shift in the absorption, which is favorable for PDT due to deeper light penetration. Finally, the biphasic dose response observed for compounds **1** and **3** is of great significance and further investigation is underway since it may be implicated in reducing the prolonged and sustained photosensitivity of such photosensitisers upon photodynamic treatment.

Conflicts of interest

There are no conflicts to declare.

Acknowledgements

The authors acknowledge support of this work by the projects "Target Identification and Development of Novel Approaches for Health and Environmental Applications" (MIS 5002514) which is implemented under the Action for the Strategic Development on the Research and Technological Sectors, and "A Greek Research Infrastructure for Visualizing and Monitoring Fundamental Biological Processes (BioImaging-GR)" (MIS 5002755) which is implemented under the Action "Reinforcement of the Research and Innovation Infrastructure". Both projects are funded by the Operational Programme "Competitiveness, Entrepreneurship and Innovation" (NSRF 2014–2020) and co-financed by Greece and the European Union (European Regional Development Fund). B. Mavroidi gratefully acknowledges financial support by Stavros Niarchos Foundation (SNF) through implementation of the program of Industrial Fellowships at NCSR "Demokritos".

References

1 P. Agostinis, K. Berg, K. A. Cengel, T. H. Foster, A. W. Girotti, S. O. Gollnick, S. M. Hahn, M. R. Hamblin, A. Juzeniene, D. Kessel, M. Korbelik, J. Moan, P. Mroz, D. Nowis, J. Piette, B. C. Wilson and J. Golab,

Photodynamic therapy of cancer: An update, *Ca-Cancer J. Clin.*, 2011, **61**, 250–281.

2 K. Plaetzer, M. Berneburg, T. Kiesslich and T. Maisch, New applications of photodynamic therapy in biomedicine and biotechnology, *BioMed Res. Int.*, 2013, **2013**, 161362.

3 Á. Juarranz, P. Jaén, F. Sanz-Rodríguez, J. Cuevas and S. González, Photodynamic therapy of cancer. Basic principles and applications, *Clin. Transl. Oncol.*, 2008, **10**, 148–154.

4 A. P. Castano, T. N. Demidova and M. R. Hamblin, Mechanisms in photodynamic therapy: part two-cellular signaling, cell metabolism and modes of cell death, *Photodiagn. Photodyn. Ther.*, 2005, **1**, 1–23.

5 C. Hopper, Photodynamic therapy: a clinical reality in the treatment of cancer, *Lancet Oncol.*, 2000, **1**, 212–219.

6 L. B. Josefsen and R. W. Boyle, Photodynamic therapy and the development of metal-based photosensitisers, *Met.-Based Drugs*, 2008, **2008**, 276109.

7 M. Salem, S. Rohani and E. R. Gillies, Curcumin, a promising anti-cancer therapeutic: a review of its chemical properties, bioactivity and approaches to cancer cell delivery, *RSC Adv.*, 2014, **4**, 10815–10829.

8 A. B. Kunnumakkara, D. Bordoloi, C. Harsha, K. Banik, S. C. Gupta and B. B. Aggarwal, Curcumin mediates anticancer effects by modulating multiple cell signaling pathways, *Clin. Sci.*, 2017, **131**, 1781–1799.

9 H. H. Tønnesen, H. de Vries, J. Karlsen and G. Beijersbergen van Henegouwen, Studies on curcumin and curcuminoids. IX: Investigation of the photobiological activity of curcumin using bacterial indicator systems, *J. Pharm. Sci.*, 1987, **76**, 371–373.

10 T. A. Dahl, W. M. McGowan, M. A. Shand and V. S. Srinivasan, Photokilling of bacteria by the natural dye curcumin, *Arch. Microbiol.*, 1989, **151**, 183–185.

11 T. Haukvik, E. Bruzell, S. Kristensen and H. H. Tønnesen, Photokilling of bacteria by curcumin in selected polyethylene glycol 400 (PEG 400) preparations. Studies on curcumin and curcuminoids, XLI, *Die Pharmazie*, 2010, **65**, 600–606.

12 L. Nardo, A. Andreoni, M. Masson, T. Haukvik and H. H. Tønnesen, Studies on curcumin and curcuminoids. XXXIX. Photophysical properties of bisdemethoxycurcumin, *J. Fluoresc.*, 2011, **21**, 627–635.

13 E. M. Bruzell, E. Morisbak and H. H. Tønnesen, Studies on curcumin and curcuminoids. XXIX. Photoinduced cytotoxicity of curcumin in selected aqueous preparations, *Photochem. Photobiol. Sci.*, 2005, **4**, 523–530.

14 L. Nardo, A. Andreoni, M. Bondani, M. Másson, T. Haukvik and H. H. Tønnesen, Studies on Curcumin and Curcuminoids. XLVI. Photophysical Properties of Dimethoxycurcumin and Bis-dehydroxycurcumin, *J. Fluoresc.*, 2012, **22**, 597–608.

15 L. Nardo, A. Andreoni, M. Bondani, M. Másson and H. Hjorth Tønnesen, Studies on curcumin and curcuminoids. XXXIV. Photophysical properties of a symmetrical, non-substituted curcumin analogue, *J. Photochem. Photobiol., B*, 2009, **97**, 77–86.

16 N. C. Araújo, C. R. Fontana, M. E. M. Gerbi and V. S. Bagnato, Overall-Mouth Disinfection by Photodynamic Therapy Using Curcumin, *Photomed Laser Surg.*, 2012, **30**, 96–101.

17 P. R. Kunwar, A. Barik, B. Mishra, K. I. Priyadarsini and K. Rathinasamy, Differential up-take and fluorescence of curcumin, a yellow pigment from turmeric, in normal vs tumor cells, *BARC Newsl.*, 2007, **285**, 202–207.

18 C. F. Chignell, P. Bilskj, K. J. Reszka, A. G. Motten, R. H. Sik and T. A. Dahl, Spectral and photochemical properties of curcumin, *Photochem. Photobiol.*, 1994, **59**, 295–302.

19 F. G. Rego-Filho, M. T. de Araujo, K. T. de Oliveira and V. S. Bagnato, Validation of Photodynamic Action via Photobleaching of a New Curcumin-Based Composite with Enhanced Water Solubility, *J. Fluoresc.*, 2014, **24**, 1407–1413.

20 A. Sreedhar, I. Sarkar, P. Rajan, J. Pai, S. Malagi, V. Kamath and R. Barmappa, Comparative evaluation of the efficacy of curcumin gel with and without photo activation as an adjunct to scaling and root planing in the treatment of chronic periodontitis: A split mouth clinical and microbiological study, *J. Nat. Sci., Biol. Med.*, 2015, **6**, 102–109.

21 N. Komerik and A. J. MacRobert, Photodynamic therapy as an alternative antimicrobial modality for oral infections, *J. Environ. Pathol., Toxicol. Oncol.*, 2006, **25**, 487–504.

22 K. I. Priyadarsini, Photophysics, photochemistry and photobiology of curcumin: Studies from organic solutions, bio-mimetics and living cells, *J. Photochem. Photobiol., C*, 2009, **10**, 81–95.

23 K. Panagiotaki, Z. Sideratou, S. Vlahopoulos, M. Paravatou-Petsotas, M. Zachariadis, N. Khoury, V. Zoumpourlis and D. Tsiourvas, Triphenylphosphonium-Functionalized Mitochondriotropic Nanocarrier for Efficient Co-Delivery of Doxorubicin and Chloroquine and Enhanced Antineoplastic Activity, *Pharmaceuticals*, 2017, **10**, 91.

24 W. Wichitnithad, U. Nimmannit, S. Wacharasindhu and P. Rojsitthisak, Synthesis, Characterization and Biological Evaluation of Succinate Prodrugs of Curcuminoids for Colon Cancer Treatment, *Molecules*, 2011, **16**, 1888–1900.

25 D. P. V. Leite, F. R. Paolillo, T. N. Parmesano, C. R. Fontana and V. S. Bagnato, Effects of Photodynamic Therapy with Blue Light and Curcumin as Mouth Rinse for Oral Disinfection: A Randomized Controlled Trial, *Photomed Laser Surg.*, 2014, **32**, 627–632.

26 K. Khorsandi, R. Hosseinzadeh and M. Fateh, Curcumin intercalated layered double hydroxide nanohybrid as a potential drug delivery system for effective photodynamic therapy in human breast cancer cells, *RSC Adv.*, 2015, **5**, 93987–93994.

27 H. Koon, A. W. N. Leung, K. K. M. Yue and N. K. Mak, Photodynamic effect of curcumin on NPC/CNE2 cells, *J. Environ. Pathol., Toxicol. Oncol.*, 2006, **25**, 205–215.
28 S. Banerjee, P. Prasad, A. Hussain, I. Khan, P. Kondaiah and A. R. Chakravarty, Remarkable photocytotoxicity of curcumin in HeLa cells in visible light and arresting its degradation on oxovanadium(IV) complex formation, *Chem. Commun.*, 2012, **48**, 7702–7704.
29 Y. J. Wang, M. H. Pan, A. L. Cheng, L. I. Lin, Y. S. Ho, C. Y. Hsieh and J. K. Lin, Stability of curcumin in buffer solutions and characterization of its degradation products, *J. Pharm. Biomed. Anal.*, 1997, **15**, 1867–1876.
30 P. Anand, A. B. Kunnumakkara, R. A. Newman and B. B. Aggarwal, Bioavailability of Curcumin: Problems and Promises, *Mol. Pharm.*, 2007, **4**, 807–818.
31 L. C. Price and R. W. Buescher, Kinetics of alkaline degradation of the food pigments curcumin and curcuminoids, *J. Food Sci.*, 2006, **62**, 267–269.
32 H. H. Tønnesen and J. Karlsen, Studies on curcumin and curcuminoids - VI. Kinetics of curcumin degradation in aqueous solution, *Z. Lebensm.-Unters. Forsch.*, 1985, **180**, 402–404.
33 M. Cozzolino, P. Delcanale, C. Montali, M. Tognolini, C. Giorgio, M. Corrado, L. Cavanna, P. Bianchini, A. Diaspro, S. Abbruzzetti and C. Viappiani, Enhanced photosensitizing properties of protein bound curcumin, *Life Sci.*, 2019, **233**, 116710.
34 M. A. Subhan, K. Alam, M. S. Rahaman, M. A. Rahman and R. Awal, Synthesis and Characterization of Metal Complexes Containing Curcumin ($C_{21}H_{20}O_6$) and Study of their Antimicrobial Activities and DNA Binding Properties, *J. Sci. Res.*, 2013, **6**, 97–109.
35 D. Patra and C. Barakat, Synchronous fluorescence spectroscopic study of solvatochromic curcumin dye, *Spectrochim. Acta, Part A*, 2011, **79**, 1034–1041.
36 H. Van Nong, L. X. Hung, P. N. Thang, V. D. Chinh, L. Van Vu, P. T. Dung, T. Van Trung and P. T. Nga, Fabrication and vibration characterization of curcumin extracted from turmeric (Curcuma longa) rhizomes of the northern Vietnam, *SpringerPlus*, 2016, **5**, 1147.
37 A. Ormond and H. Freeman, Dye Sensitizers for Photodynamic Therapy, *Materials*, 2013, **6**, 817–840.
38 G. Jori, Tumour photosensitizers: approaches to enhance the selectivity and efficiency of photodynamic therapy, *J. Photochem. Photobiol., B*, 1996, **36**, 87–93.
39 R. Jagannathan, P. M. Abraham and P. Poddar, Temperature-Dependent Spectroscopic Evidences of Curcumin in Aqueous Medium: A Mechanistic Study of Its Solubility and Stability, *J. Phys. Chem. B*, 2012, **116**, 14533–14540.
40 K. Priyadarsini, The Chemistry of Curcumin: From Extraction to Therapeutic Agent, *Molecules*, 2014, **19**, 20091–20112.
41 M. Kharat, Z. Du, G. Zhang and D. J. McClements, Physical and Chemical Stability of Curcumin in Aqueous Solutions and Emulsions: Impact of pH, Temperature, and Molecular Environment, *J. Agric. Food Chem.*, 2017, **65**, 1525–1532.
42 M. Ghosh, A. T. K. Singh, W. Xu, T. Sulchek, L. I. Gordon and R. O. Ryan, Curcumin nanodisks: formulation and characterization, *Nanomedicine*, 2011, **7**, 162–167.
43 R. Bonnett and G. Martínez, Photobleaching of sensitisers used in photodynamic therapy, *Tetrahedron*, 2001, **57**, 9513–9547.
44 D. Deeb, Y. X. Xu, H. Jiang, X. Gao, N. Janakiraman, R. A. Chapman and S. C. Gautam, Curcumin (diferuloylmethane) enhances tumor necrosis factor-related apoptosis-inducing ligand-induced apoptosis in LNCaP prostate cancer cells, *Mol. Cancer Ther.*, 2003, **2**, 95–103.
45 A. Petri, D. Yova, E. Alexandratou, M. Kyriazi and M. Rallis, Comparative characterization of the cellular uptake and photodynamic efficiency of Foscan® and Fospeg in a human prostate cancer cell line, *Photodiagn. Photodyn. Ther.*, 2012, **9**, 344–354.
46 V. Ellerkamp, N. Bortel, E. Schmid, B. Kirchner, S. Armeanu-Ebinger and J. Fuchs, hotodynamic Therapy Potentiates the Effects of Curcumin on Pediatric Epithelial Liver Tumor Cells, *Anticancer Res.*, 2016, **36**, 3363–3372.
47 Z. Hussain, H. E. Thu, M. W. Amjad, F. Hussain, T. A. Ahmed and S. Khan, Exploring recent developments to improve antioxidant, anti-inflammatory and antimicrobial efficacy of curcumin: A review of new trends and future perspectives, *Mater. Sci. Eng., C*, 2017, **77**, 1316–1326.
48 A. S. Martirosyan, H. R. Vardapetyan, S. G. Tiratsuyan and A. A. Hovhannisyan, Biphasic dose–response of antioxidants in hypericin-induced photohemolysis, *Photodiagn. Photodyn. Ther.*, 2011, **8**, 282–287.
49 M. Tanaka, M. Kinoshita, Y. Yoshihara, N. Shinomiya, S. Seki, K. Nemoto, M. R. Hamblin and Y. Morimoto, Photodynamic therapy using intra-articular Photofrin for murine MRSA arthritis: biphasic light dose response for neutrophil-mediated antibacterial effect, *Lasers Surg. Med.*, 2011, **43**, 221–229.
50 M. Tanaka, P. Mroz, T. Dai, M. Kinoshita, Y. Morimoto and M. R. Hamblin, Photodynamic therapy can induce non-specific protective immunity against a bacterial infection, *Proc. SPIE 8224, Biophotonics Immun. Respons. VII*, 2012, **8224**, 822403.
51 A. P. Castano, T. N. Demidova and M. R. Hamblin, Mechanisms in photodynamic therapy: part one-photosensitizers, photochemistry and cellular localization, *Photodiagn. Photodyn. Ther.*, 2004, **1**, 279–293.
52 A. A. Rosenkranz, D. A. Jans and A. S. Sobolev, Targeted intracellular delivery of photosensitizers to enhance photodynamic efficiency, *Immunol. Cell Biol.*, 2000, **78**, 452–464.
53 H. Abrahamse and M. R. Hamblin, New photosensitizers for photodynamic therapy, *Biochem. J.*, 2016, **473**, 347–364.
54 S. Jiang, R. Zhu, X. He, J. Wang, M. Wang, Y. Qian and S. Wang, Enhanced photocytotoxicity of curcumin delivered by solid lipid nanoparticles, *Int. J. Nanomed.*, 2016, **12**, 167–178.
55 A. Kunwar, A. Barik, B. Mishra, K. Rathinasamy, R. Pandey and K. I. Priyadarsini, Quantitative cellular uptake,

localization and cytotoxicity of curcumin in normal and tumor cells, *Biochim. Biophys. Acta*, 2008, **1780**, 673–679.

56 S. Ben-Zichri, S. Kolusheva, M. Danilenko, S. Ossikbayeva, W. J. Stabbert, J. L. Poggio, D. E. Stein, Z. Orynbayeva and R. Jelinek, Cardiolipin mediates curcumin interactions with mitochondrial membranes, *Biochim. Biophys. Acta, Biomembr.*, 2019, **1861**, 75–82.

57 A. Moustapha, P. Pérétout, N. Rainey, F. Sureau, M. Geze, J.-M. Petit, E. Dewailly, C. Slomianny and P. Petit, Curcumin induces crosstalk between autophagy and apoptosis mediated by calcium release from the endoplasmic reticulum, lysosomal destabilization and mitochondrial events, *Cell Death Discovery*, 2015, **26**, 15017.